Forest Ecology and Management 430 (2018) 346–356

Contents lists available at ScienceDirect

Forest Ecology and Management

journal homepage: www.elsevier.com/locate/foreco

Rainfall thresholds for post-fire runoff and sediment delivery from plot to watershed scales

Codie Wilson[a,*], Stephanie K. Kampf[b], Joseph W. Wagenbrenner[c], Lee H. MacDonald[d]

[a] Department of Geosciences, 1482 Campus Delivery, Colorado State University, Fort Collins, CO 80523-1482, United States
[b] Department of Ecosystem Science and Sustainability, 1476 Campus Delivery, Colorado State University, Fort Collins, CO 80523-1476, United States
[c] USDA Forest Service, Pacific Southwest Research Station, Arcata, CA 95521, United States
[d] Natural Resource Ecology Laboratory, 1499 Campus Delivery, Colorado State University, Fort Collins, CO 80523-1499, United States

ARTICLE INFO

Keywords:
Rainfall frequency
Post-fire runoff
Post-fire erosion
Mulch treatments
Colorado Front Range
Spatial scale

ABSTRACT

Wildfire increases the likelihood of runoff, erosion, and downstream sedimentation in many of the watersheds that supply water for Colorado's Front Range communities. The objectives of this study were to: (1) identify rainfall intensity thresholds for a post-fire runoff or sediment delivery response at plots (≤0.06 ha), hillslopes (0.07–5.2 ha) and watersheds (100–1500 ha) after three Colorado Front Range wildfires for up to four years post-fire; (2) determine how the rainfall thresholds varied by fire location, year post-fire, spatial scale, and mulch treatments; and (3) use long-term rainfall data to map the likely frequency of rainfall events above these intensity thresholds as an indicator of risk for post-fire runoff or sediment delivery from future high severity fires in Colorado. Maximum 60-min rainfall intensity (MI_{60}) thresholds were identified as the values that best separated rain storms that generated responses from those that did not. We found that thresholds did not significantly differ among fires for any year post-fire. Thresholds did significantly vary among spatial scales; for the first two years post-fire, high-confidence thresholds ranged from 4 to 8 mm h^{-1} across unmulched plots, hillslopes and watersheds. Compared to post-fire year 0, thresholds in year 3 were significantly higher, with high-confidence thresholds up to 22 mm h^{-1}. NOAA Atlas rainfall data were used to compute and map frequencies of threshold exceedance across Colorado. Within the Front Range study area, rain storms with MI_{60} of 4 mm h^{-1} have frequencies ranging from 5 to 11 times per summer, while MI_{60} values of 8 mm h^{-1} have frequencies of 2–5 times per summer. Maps of threshold exceedance frequency can help identify areas most vulnerable to post-fire runoff and sediment delivery and prioritize post-fire emergency planning.

1. Introduction

In the western United States, higher temperatures and earlier spring snowmelt have increased the frequency and duration of large wildfires (Westerling et al., 2006; Litschert et al., 2012). After a wildfire, runoff and erosion can be up to several orders of magnitude higher than pre-fire conditions (e.g., Larsen et al., 2009; Noske et al., 2016; Wagenbrenner and Robichaud, 2014); this can lead to difficulties for both emergency management and water treatment, such as flooding and delivery of sediment, ash and other constituents to streams (Hohner et al., 2016; Martin, 2016).

In the Colorado Front Range, post-fire runoff and erosion are almost exclusively driven by summer thunderstorms and subsequent infiltration-excess (Hortonian) overland flow (Benavides-Solorio and MacDonald, 2005; Moody et al., 2013; Wagenbrenner and Robichaud, 2014). The generation of infiltration-excess overland flow exhibits threshold behavior, as high rainfall intensities are needed to exceed the infiltration capacities of soils and generate runoff on plots or hillslopes.

Rainfall thresholds for post-fire response (defined here as runoff or sediment delivery) vary with fire severity, time since burning and soil type (Benavides-Solorio and MacDonald, 2005; Miller et al., 2011). The lowest thresholds are immediately after a high severity fire due to the loss of surface cover, decrease in soil organic matter, and exposure of the soils to raindrop impact and soil sealing (Moody and Martin, 2001a; Larsen et al., 2009). Previous research on plots and hillslopes (≤5.2 ha) has shown that post-fire mulch treatments and vegetation regrowth increase surface cover, surface roughness, and rainfall interception, thereby protecting soil from raindrop impact, slowing overland flow, and reducing runoff and erosion (Wagenbrenner et al., 2006; Robichaud et al., 2013a,b; Wainwright et al., 2000; Moreno-de las Heras et al., 2010; Inbar et al., 1998).

While the factors affecting post-fire runoff and erosion on plots and

* Corresponding author.
E-mail address: Codie.Wilson@colostate.edu (C. Wilson).

https://doi.org/10.1016/j.foreco.2018.08.025
Received 3 November 2017; Received in revised form 10 August 2018; Accepted 12 August 2018
Available online 23 August 2018
0378-1127/

hillslopes are relatively well-documented, predicting post-fire runoff and sediment delivery for watersheds remains difficult due to high variability in rainfall, burn severity, soil properties and topography (Moody et al., 2008; Kutiel et al., 1995). This increasing variability with larger drainage area generally causes thresholds to increase (Cammeraat, 2002; Cammeraat, 2004) due to longer flow paths (Wagenbrenner and Robichaud, 2014) that allow more opportunities for water infiltration and storage.

After a fire, the production of infiltration-excess overland flow reduces over time and typically only the most extreme storms generate overland flow by three to four years after burning (Ebel and Martin, 2017; Moody and Martin, 2001a; Wagenbrenner et al., 2015). As recovery conditions and rates may vary among fire locations and responses of interest (e.g., runoff or sediment delivery), modeling specific complex hydrological processes remains difficult, particularly across spatial scales. However, approaches that simplify interactions between fire, rainfall and landscape properties may be more important than the exact hydrologic transfer processes that occur in a recovering landscape (Nyman et al., 2013).

Rainfall thresholds can be used to integrate complex processes into a single comparable metric for predicting the frequency of post-fire runoff and sediment delivery without having to rely on more complex process-based models. Comparing thresholds between spatial scales, fires, and post-fire treatments is useful for interpreting the hydrologic processes and scale-effects that emerge with post-fire mulch treatments and recovery. Therefore, the goal of this study is to provide information on post-fire thresholds for runoff and sediment delivery across multiple fires, years post-fire, spatial scales, and mulch treatments in the Colorado Front Range. Specific objectives are to:

1. Identify rainfall intensity thresholds for a post-fire runoff or sediment delivery response at plots ($\leq$0.06 ha), hillslopes (0.07–5.2 ha) and watersheds (100–1500 ha) after three Colorado Front Range wildfires for up to four years post-fire;
2. Determine how rainfall thresholds varied by fire location, year post-fire, spatial scale, and mulch treatments;
3. Use long-term rainfall data to map the likely frequency of rainfall events above these intensity thresholds as an indicator of risk for post-fire runoff or sediment delivery from future high severity fires in Colorado.

2. Materials and methods

2.1. Site descriptions and sample sizes

Post-fire rainfall, runoff and sediment delivery data were compiled for three Colorado Front Range wildfires: the 2000 Bobcat fire (Wagenbrenner et al., 2006; Wagenbrenner and Robichaud, 2014; Kunze and Stednick, 2006), the 2002 Hayman fire (Robichaud et al., 2013a,b, 2008; Wagenbrenner and Robichaud, 2014), and the 2012 High Park fire (This study; Schmeer, 2014; S. Ryan, USFS, unpublished data; Fig. 1). These fires were selected because they each had relatively detailed rainfall data linked with either runoff or sediment delivery data for at least three years post-fire and two or more spatial scales.

Elevations of the study sites within these fires ranged from 1700 to 2700 m. Climate within the study area is semiarid and monsoonal with 60–75% of the annual 400–600 mm of precipitation occurring as rain during the spring and summer months (April - September; PRISM Climate Group 2018). The primary pre-fire vegetation was ponderosa pine (*Pinus ponderosa*) at lower elevations and denser mixed conifer forests at higher elevations, with grasses and shrubs on drier south-facing slopes (BAER, 2012; Robichaud et al., 2013b; Kunze and Stednick, 2006; Schmeer et al., 2018). Soils are derived from granitic (Robichaud et al., 2013b; Schmeer et al., 2018) and metasedimentary parent materials (Braddock et al., 1970). The dominant soil type in the Bobcat and High Park fires is sandy loam, whereas soil in the Hayman

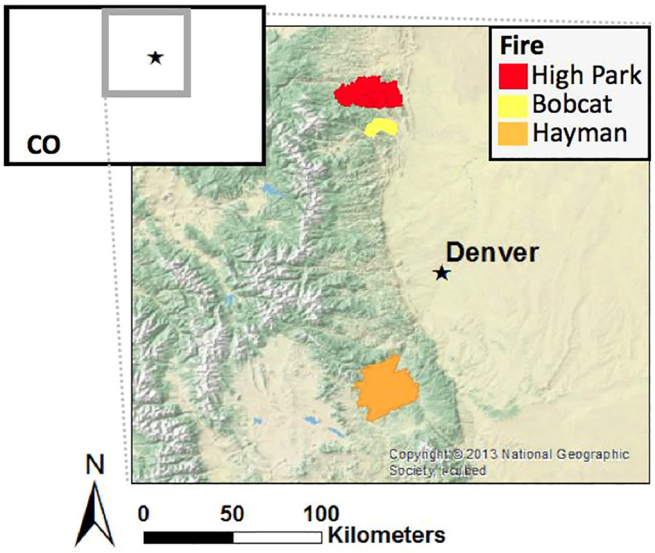

Fig. 1. Location of the three Colorado Front Range fires used in this analysis; from north to south, they are the 2012 High Park fire, the 2000 Bobcat fire, and the 2002 Hayman fire. Imagery from ESRI (2013). Maps produced using GCS WGS 1984.

fire is gravelly coarse sand (Robichaud et al., 2013a; Wagenbrenner and Robichaud, 2014; BAER, 2012).

We classified each monitoring site as a plot, hillslope or watershed. Plots were typically on planar slopes with an area of $\leq$0.06 ha in which sediment fences were used to measure sediment delivery (cf. Robichaud and Brown, 2002). Data were available for eleven plots within the Bobcat fire and 32 plots within the Hayman fire (Table 1). The Bobcat, Hayman and High Park fires each had 23–32 hillslopes, defined here as ephemeral, convergent swales or headwater channels with contributing areas of 0.07–5.2 ha. Sediment fences or larger sediment traps were used to measure hillslope sediment delivery. In both plots and hillslopes, sediment fences were cleaned out after major storms to measure deposited sediment mass. At the watershed scale of 100–1500 ha, runoff responses were measured at two watersheds within the Bobcat fire and six watersheds within the High Park fire (Table 1).

Site characteristics and treatments to mitigate post-fire responses varied by spatial scale. Plots and hillslopes were generally placed in locations burned at high severity, whereas watersheds covered larger areas and therefore had combinations of moderate and high severity. Average slopes by spatial scale were 17° for planar plots, 15° for the convergent hillslopes, and 17° for watersheds. Treatments included straw mulch, contour felling, straw wattles, and aerial seeding in the Bobcat fire; straw mulch, hydromulch, wood mulch, contour felling, and aerial seeding in the Hayman fire; and straw and wood-shred mulch in the High Park fire. Aerial seeding in parts of the Bobcat and Hayman fires did not significantly affect vegetation regrowth or post-fire sediment delivery rates (Wagenbrenner et al., 2006; Rough, 2007). Contour felled logs at two plots in the Bobcat fire and one hillslope in the Hayman fire also did not significantly reduce sediment yields (Wagenbrenner et al., 2006; Robichaud et al., 2008). Because mulch was the most common treatment used across all fires, we chose to consider only the effects of mulch treatments on thresholds. We stratified sites by the presence or absence of mulch rather than the extent of mulch cover because the extent and type of mulch varied widely, and not all locations had data on the amount of mulch cover over time. One Bobcat plot and 16 Hayman plots were mulched. For hillslopes, 6 Bobcat, 11 Hayman, and 9 High Park fire sites were mulched (Table 1). Mulch was applied to 0–16% (average = 8%) of the watershed areas in the Bobcat fire (Kunze and Stednick, 2006) and 1–77% (average = 22%) of the watershed areas in the High Park fire. We chose

Table 1
Spatial scale, contributing area, total number of sites (with number mulched in parentheses), years monitored post-fire, and references for the data from each of the three fires used in this study.

Fire, Year	Spatial scale	Area (ha)	No. of sites (no. mulched)	Years post-fire	Reference
Bobcat, 2000	Plot	≤0.06	11 (1)	0–3	Wagenbrenner et al. (2006)
	Hillslope	0.07–5.2	23 (6)	0–3	Wagenbrenner and Robichaud (2014)
	Watershed	100–1500	2	0–2	Kunze and Stednick (2006)
Hayman, 2002	Plot	≤0.06	32 (16)	1–4	Robichaud et al. (2013a)
	Hillslope	0.07–5.2	32 (11)	0–4	Robichaud et al. (2008), Wagenbrenner and Robichaud (2014); Robichaud et al. (2013b)
High Park, 2012	Hillslope	0.07–5.2	31 (9)	0–3	This study; Schmeer (2014)
	Watershed	100–1500	6	2–4	This study; S. Ryan, US Forest Service, unpublished data

not to consider the effects of mulch at the watershed scale because the areas mulched were generally small fractions of the watershed areas.

2.2. Observations of rainfall, runoff or sediment delivery

We included observations of rainfall, runoff or sediment delivery from the summer thunderstorm season of June-September because this is when nearly all post-fire sediment delivery from plots and hillslopes occurs in this region (e.g., Benavides-Solorio and MacDonald, 2005). Post-fire summers and years were numbered consecutively, with 0 representing the year of the fire. Most plot and hillslope data extended from year 0 through at least post-fire year 3. Watershed data were collected for post-fire years 0–2 in the Bobcat fire and post-fire years 2–4 in the High Park fire (Table 1).

Tipping bucket rain gauges were located within or relatively near (100–2500 m) each plot, hillslope and watershed. Rainfall events recorded by the gauges were identified using the USDA Rainfall Intensity Summarization Tool (RIST; ARS, 2013). Rain storms were separated by a period of at least 6 h with < 1 mm of rain (Renard et al., 1997). The following rainfall metrics were calculated for each rain storm: depth (mm); maximum intensity (mm h^{-1}) over 5-, 15-, 30-, and 60-min intervals (MI_5, MI_{15}, MI_{30} and MI_{60}); and erosivity (EI_{30}).

To determine which rainfall metric to use in the threshold analysis, the ability of different rainfall metrics to predict runoff or sediment delivery was tested using a nominal logistic model. MI_{15}, EI_{30} and MI_{60} were the best rainfall metrics to predict a response ($p < 0.0001$). We chose to identify thresholds with MI_{60} because hourly rainfall data are more commonly available than finer time step data.

Runoff at plots and hillslopes was ephemeral, only occurring during and immediately after rain storms. The time intervals for inspecting and cleaning out the sediment fences varied, but all sites were visited multiple times each summer. For two hillslopes in the Hayman fire and four hillslopes in the High Park fire runoff was continuously monitored using sediment traps with stage recorders (Robichaud et al., 2013b); these concurrent measurements of runoff and sediment delivery showed that sediment only accumulated in the sediment fences during storms that generated runoff. For locations without continuous runoff monitoring we could therefore assume that the presence of sediment in the fence indicated that runoff had occurred. All watersheds had perennial flow, and in most cases stream stage was continuously monitored with either capacitance rods (TruTrack WT-HR 1000 mm, Auckland, NZ) or pressure transducers (Model PDCR 1230 Druck) and data loggers (CR10X Campbell Scientific Inc., Logan, UT); indirect estimates based on high water marks were used for Bobcat watersheds in year 0 (Kunze and Stednick, 2006). Stage-discharge relationships were developed for each site using manual velocity measurements; runoff responses to rain events were identified as rises in streamflow above baseflow following Kunze and Stednick (2006).

For each rain storm, we determined if there had been a response of either runoff or sediment delivery. If multiple rain storms occurred between site visits or if multiple rain gauges were associated with a site, the rain storm or gauge with the highest EI_{30} was linked to the observed response (e.g., Benavides-Solorio and MacDonald, 2005). Rainfall events with no observed response, including multiple rainfall events between site visits, were designated as no response. The varying intervals between site visits for the plots and hillslopes causes some uncertainty about which rainfall event generated a given response. We evaluated the extent to which our procedure biased the results using Spearman's rank correlation coefficient (r) between EI_{30} and the magnitude of runoff (mm) or sediment yields (Mg ha^{-1}) for sites with continuous monitoring (watersheds in Bobcat and High Park fires and select hillslopes within the Hayman and High Park fires). The magnitudes of runoff and sediment yields were positively related to EI_{30} (Spearman's $r = 0.57$ and 0.54; $p < 0.0001$; $n = 132$ and 64, respectively), indicating that selecting the event with the highest EI_{30} between site visits is a reasonable approach for determining which rain storm to associate with each response.

2.3. Threshold identification and assessment

All rain storms with their associated presence or absence of a response were compiled into sample groups by fire (n = 3), year post-fire (n ≤ 5), spatial scale (n ≤ 3) and presence or absence of mulch treatments. We did not stratify by slope because prior research on these fires showed that slope did not significantly affect sediment yields (Wagenbrenner et al., 2006; Wagenbrenner and Robichaud, 2014; Schmeer et al., 2018). Altogether this resulted in 48 distinct sample groups (Table 2).

For each sample group, we identified thresholds as the MI_{60} value(s) that maximized the fraction (*F*) of rainfall events for which a response was correctly predicted using:

$$F = \frac{TP + TN}{P} \quad (1)$$

where *TP* was the number of true positives, defined as rainfall events with MI_{60} greater than or equal to the identified threshold with an observed response; *TN* was the number of true negatives, defined as rain storms with MI_{60} less than the identified threshold with no observed response, and *P* was the total number of rainfall events for that sample group. In most cases, more than one MI_{60} value produced the maximum *F* value; for these, we identified the minimum MI_{60} value (T_{min}) and the maximum MI_{60} value (T_{max}). Threshold prediction errors were either false positives (*FP*) or false negatives (*FN*). *FP* were storms without an observed response but with an MI_{60} greater than T_{min}, and *FN* were storms with an observed response but with an MI_{60} less than T_{min}.

The agreement between predicted and observed responses was evaluated by Cohen's kappa statistic (κ):

$$\kappa = \frac{F - p_e}{1 - p_e} \quad (2)$$

where *F* was defined in Eq. (1) and p_e was the hypothetical probability

Table 2
Number of summer rain storms and percent with runoff or sediment delivery (Y) for unmulched and mulched (N/Y) plots, hillslopes and watersheds by year post-fire fire, and spatial scale. Blank cells indicate no data.

Spatial scale:			Plot		Hillslope		Watershed	
Year	Fire	Mulch	No. of rain storms	Y (%)	No. of rain storms	Y (%)	No. of rain storms	Y (%)
0	Bobcat	N	80	10	78	24	22	18
		Y	2	100	35	14		
	Hayman	N			1232	6		
		Y			143	3		
	High Park	N			94	24		
		Y			22	23		
1	Bobcat	N	210	14	384	21	50	40
		Y	25	16	135	11		
	Hayman	N	268	18	368	27		
		Y	268	12	298	13		
	High Park	N			387	22		
		Y			178	9		
2	Bobcat	N	110	22	223	12	28	7
		Y	15	13	70	6		
	Hayman	N	534	13	957	10		
		Y	528	11	365	12		
	High Park	N			598	11	155	8
		Y			221	11		
3	Bobcat	N	150	2	255	2		
		Y	15	0	90	0		
	Hayman	N	442	4	37	3		
		Y	442	4	26	4		
	High Park	N			486	5	253	11
		Y			178	9		
4	Hayman	N	438	16	40	3		
		Y	438	15	37	3		
	High Park	N					112	13

of chance agreement computed as:

$$p_e = p_{o,Y} * p_{t,Y} + p_{o,N} * p_{t,N} \quad (3)$$

where p_o is the fraction of observed responses and p_t is the fraction of responses predicted by T_{min}. The Y subscript indicates a response, while N indicates no response. κ can range from −1 to 1 with values of 0.41–0.60 indicating moderate agreement, 0.61–0.80 indicating substantial agreement, and 0.81–0.99 indicating almost perfect agreement (Viera and Garrett, 2005). We use κ values ≥0.61 to indicate high-confidence in a given threshold.

2.4. Effects of fire location, year post-fire, spatial scale, and mulch treatments on thresholds

Comparisons among sample groups were used to evaluate whether fire location, year post-fire, spatial scale or mulch treatments affected the threshold values. We first computed four separate ANOVAs because a single ANOVA applied to the full dataset simultaneously had insufficient degrees of freedom. For the first two ANOVAs, we assessed the effects of mulch treatments on T_{min} for (1) plots and (2) hillslopes with fire location, year post-fire and mulch presence/absence as fixed effects (JMP Version 12.0.1); only plots and hillslopes were included in the first two ANOVAs because we did not stratify watersheds by mulch presence/absence. The first two ANOVAs indicated that mulch was not a significant fixed effect, so we conducted a third ANOVA for all spatial scales assessing fire location, year post-fire, and spatial scale as fixed effects on T_{min}. Fire location was an insignificant fixed effect in each of the first three ANOVAs, so we conducted a final ANOVA assessing year post-fire, spatial scale and interactions between year and spatial scale as fixed effects on $T_{min.}$ Pairwise differences among significant fixed effects for all models were further examined using Tukey's HSD (JMP Version 12.0.1).

We also examined differences in T_{min} between sample groups to assess the effects of fire location, year post-fire, spatial scale and mulch treatments; these comparisons did not involve statistical tests. For fire location, we compared T_{min} for unmulched hillslopes in post-fire years 0–3 among each of the three fires. We used the unmulched hillslopes for this comparison because this was the most extensive dataset common to all three fires. To examine the effect of year post-fire, we compared T_{min} for each year post-fire stratifying by fire, spatial scale, and the presence or absence of mulch. The effect of spatial scale was evaluated by comparing T_{min} for each year and fire across the spatial scales for which data were available (Table 1). Finally, the effect of mulch was evaluated for plots and hillslopes by comparing thresholds for sites with and without mulch when stratified by fire, year post-fire, and spatial scale.

The effect of antecedent precipitation on thresholds was also assessed for watersheds with perennial flow, continuous monitoring, and high-confidence thresholds. For this, we used High Park fire watershed scale data for post-fire years 2–4 (n = 520); watershed scale data from the Bobcat fire for years 0–2 (n = 99) were excluded because continuous monitoring was not available in post-fire year 0 (Kunze and Stednick, 2006), and confidence was low in post-fire years 1–2. We calculated the daily antecedent precipitation index (I_a) as:

$$I_a = I_o k + I \quad (4)$$

where I_o was the initial value of I_a, I was the rainfall on a given day, and k the recession factor set to 0.9 (Dingman, 2002). We compared differences in I_a between rain storms with and without runoff responses across all six watersheds using ANOVA. Our significance level for all analyses and results was 0.05.

2.5. Threshold frequency maps

The frequencies of rain storms in Colorado with intensities equal to or greater than the MI_{60} thresholds were computed using data from the 47 NOAA stations with 25–39 years of 15-min rainfall data (Perica et al., 2013). We used data from the summer thunderstorm season (June-September) and excluded summers missing more than 14 days of data to minimize underestimation of event frequencies. Rain storms with MI_{60} less than 3 mm h^{-1} were also excluded because these values were below the precision of most NOAA rain gauges. The remaining rainfall events for each station were ranked over the period of record by MI_{60}, and the frequency of occurrence for each rain storm was computed by:

$$Frequency = \frac{rank}{(n+1)} \quad (5)$$

where *rank* is an integer and *n* is the number of summers with rainfall data.

The calculated MI_{60} frequencies allowed us to determine the average number of times that the MI_{60} from summer rain storms would equal or exceed a given MI_{60} threshold. For each NOAA station, a polynomial was fit to MI_{60} values plotted against calculated MI_{60} frequencies (Eq. (5)) for rain storms of 4–12 mm h^{-1}. We chose this range because most higher intensities are already mapped in the NOAA Atlas. Rain storm frequencies were spatially interpolated in 1 mm h^{-1} increments from 4 to 12 mm h^{-1} over the state of Colorado by co-kriging the calculated frequencies from the 47 stations with the mean June-September rainfall as estimated for 1981–2010 using Parameter-elevation Relationships on Independent Slopes Model (PRISM) data (PRISM Climate Group, 2017). The inclusion of PRISM rainfall helped to smooth edges and fill in spatial gaps among the 47 stations.

The density of NOAA stations used in this analysis was lower in northwestern Colorado than in central and eastern Colorado. To limit uncertainty, we focused the frequency analysis on the fire-prone eastern slope of the Colorado Front Range (Veblen et al., 2000), where our study fires occurred. For this region, we determined how the frequency

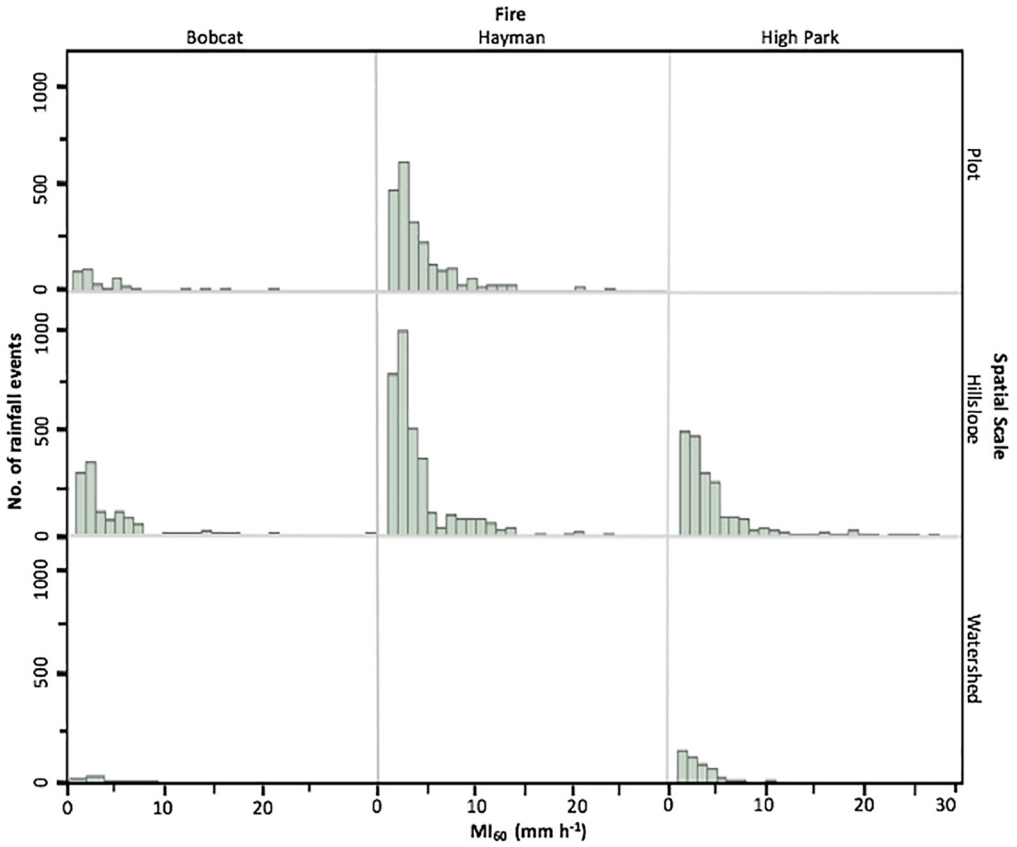

Fig. 2. Histograms of MI_{60} rainfall events in increments of 2 mm h^{-1} by fire and spatial scale. Blank cells indicate no data.

of events in the range of 4–12 mm h^{-1} varied with elevation.

3. Results

3.1. Number and magnitude of rainfall events

The total number of site-rain events was 11,522, but the sample size varied greatly by spatial scale and fire (Table 2). Overall, more than 94% of the rain storms in the dataset were for plot and hillslope scales (Fig. 2). The Hayman fire accounted for 85% of the rain storms at the plot scale and 50% of the storms at the hillslope scale. Slightly less than 6% of the rain storms were recorded at the watershed scale, and 84% of these were from the High Park fire (Fig. 2). In a given year, the percent of rain storms that produced a response ranged from 0 to 100% for plots (average across years = 17%), 0–24% for hillslopes (average = 11%), and 7–40% for watersheds (average = 16%; Table 2). MI_{60} values for most rain storms were very low (Fig. 2), with median values generally from 2 to 5 mm h^{-1} for a given fire, year post-fire and spatial scale. The maximum MI_{60} values for the different sample groups ranged from 5 to 31 mm h^{-1}, with most values ranging from 10 to 23 mm h^{-1}.

3.2. Effects of fire location, year post-fire, spatial scale, and mulch treatments on thresholds

Overall, thresholds ranged from 2 to 31 mm h^{-1}, and prediction accuracy (*F*) for minimum thresholds (T_{min}) was high, averaging 0.92 (Table 3, Fig. 3). Agreement between predictions and observations was not as strong; κ for T_{min} ranged from −0.51 to 1 with an average of 0.54. The percent of summer storms resulting in threshold prediction errors ranged from 0 to 50% (average = 4%), with more false positives (average = 5%) than false negatives (average = 2%) (Table S1). For post-fire years 0–2, high-confidence T_{min} values ($\kappa \geq 0.61$) were 4–8 mm h^{-1} across all spatial scales (average = 7 mm h^{-1}). Thresholds increased to a range of 7–22 mm h^{-1} in post-fire year 3 (average = 10 mm h^{-1}). High-confidence thresholds in post-fire year 4 were 5–6 mm h^{-1}, but these only represent plots in the Hayman fire and watersheds in the High Park fire.

The first two ANOVAs with fire location, year post-fire and mulch presence/absence as fixed effects on T_{min} revealed nearly significant ($p = 0.06$) and significant effects ($p = 0.02$) of year post-fire for plots and hillslopes, respectively (Table 4). Fire location and mulch treatments were not significant fixed effects. Subsequent pairwise comparisons (Tukey's HSD) of year post-fire for the hillslope model revealed significant differences between: (1) years 0 and 4, and (2) years 1 and 4 ($p = 0.01$ and 0.05, respectively) (Table S2). The third ANOVA with fire location, year post-fire, and spatial scale as fixed effects on T_{min} showed significant effects of year post-fire ($p = 0.01$) and spatial scale ($p = 0.01$) (Table 4). Pairwise comparisons for the third model indicated that T_{min} across all fires and spatial scales was significantly greater for post-fire year 3 than year 0. The final ANOVA with year post-fire, spatial scale, and interactions of year post-fire and spatial scale as fixed effects on T_{min} identified only spatial scale as significant ($p = 0.01$).

The comparison of threshold ranges between sample groups helps illustrate why the ANOVA models did or did not show significant differences in thresholds. First, mulch was not found to be a statistically significant effect on threshold values for the plot and hillslope models (Table 4), which may be because the effects of mulch varied by fire, spatial scale and year post-fire (Fig. 4). Within the Bobcat fire, confidence in threshold predictions for plots in years 0 and 3 was low, and T_{min} was similar for both mulched and unmulched plots (Table 3). For Bobcat hillslopes, confidence in both the mulched and unmulched thresholds was high only in post-fire year 1, when the T_{min} was 7 mm h^{-1} for unmulched and 11 mm h^{-1} for mulched hillslopes (Table 3). In post-fire year 3, both the unmulched and mulched hillslopes in the Bobcat fire had T_{min} values of 22 mm h^{-1} (Table 3). In the

Table 3
MI_{60} rainfall thresholds (T_{min} and T_{max}; mm h^{-1}) for unmulched and mulched (N/Y) plots, hillslopes, and watersheds by year post-fire, fire and spatial scale with the fraction (*F*) of rain storms that correctly predicted a response of runoff or sediment delivery, and corresponding kappa statistic (κ). Blank cells indicate no data.

Spatial scale:			Plot				Hillslope				Watershed			
Year	Fire	Mulch	T_{min}	T_{max}	*F*	κ	T_{min}	T_{max}	*F*	κ	T_{min}	T_{max}	*F*	κ
0	Bobcat	N	7.6	7.6	0.9	0	6.8	7.5	0.88	0.67	6.8[b]	7.5	0.86	0.58
		Y	5.4[a]	31.3	0.5	0	7.6	31.2	0.89	−0.51				
	Hayman	N					10.9	11.1	0.96	0.57				
		Y					11.2	11.2	0.97	0				
	High Park	N					4.1	4.3	0.88	0.69				
		Y					3.5	4	0.95	0.88				
1	Bobcat	N	6.6	7.7	0.95	0.77	6.6	6.7	0.87	0.82	2	3.3	0.6	0.22
		Y	6.8[b]	7.4	0.88	0.5	11.1	13.5	0.92	0.55				
	Hayman	N	8.1	9.1	0.99	0.97	9.3	9.7	0.85	0.58				
		Y	8.1	9.1	1	1	11	11.1	0.9	0.5				
	High Park	N					6.9	7.3	0.88	0.7				
		Y					16.6	18.5	0.93	0.51				
2	Bobcat	N	4.4	6.1	0.96	0.89	7.3	7.7	0.93	0.76	12[b]	12	0.93	0
		Y	7.3[b]	7.7	0.93	0.63	12	12	0.94	−0.43				
	Hayman	N	5.4	5.6	0.95	0.8	7.9	9.5	0.94	0.69				
		Y	5.4	5.6	0.95	0.8	8	8.2	0.93	0.7				
	High Park	N					12	15.6	0.92	0.45	8.4	10.4	0.98	0.86
		Y					17.1	18	0.92	0.43				
3	Bobcat	N	21.5	21.5	0.98	0	21.5	21.5	0.98	0.61				
		Y	17.8[b]	17.8	1	[c]	21.5	21.5	1	[c]				
	Hayman	N	7.7	7.7	1	1	7.9	9.5	1	1				
		Y	7.7	7.7	1	1	7.7[b]	7.9	0.96	0.65				
	High Park	N					12	12.6	0.97	0.52	7.4	10.1	0.96	0.74
		Y					10.2	10.6	0.94	0.64				
4	Hayman	N	6.2	6.3	0.92	0.75	20.6	20.6[c]	0.98	0				
		Y	6.2	6.3	0.92	0.73	20.6	20.6[c]	0.97	0				
	High Park	N									5	5.7	0.92	0.68

[a] Sample size ≤ 10.
[b] Sample size ≤ 30.
[c] κ could not be calculated because all events predicted to have no flow.

Hayman fire, thresholds were similar for mulched and unmulched plots and hillslopes (Table 3). In the High Park fire, during post-fire year 1, the mulched hillslopes had a T_{min} of 17 mm h^{-1}, more than twice the value of the unmulched hillslopes, but differences between the mulched and unmulched hillslope thresholds decreased in post-fire year 2 and became negligible in year 3 (Table 3). In summary, mulch treatments did increase the T_{min} values in a few cases, but in most comparisons by fire and year post-fire, T_{min} values were similar for mulched and unmulched sites.

Fire location also did not emerge as a significant fixed effect in the

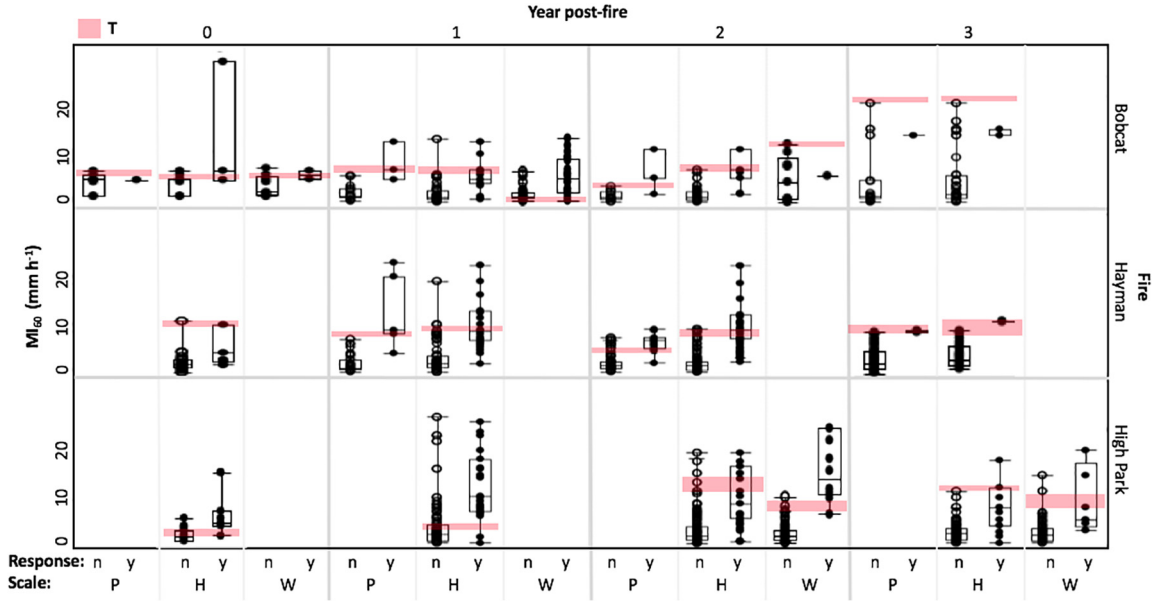

Fig. 3. MI_{60} rainfall and thresholds (T) for unmulched sites by year post-fire, fire location, spatial scale, and response absence (n; open circles) or presence (y; filled circles). Spatial scale abbreviations are plots (P), hillslopes (H) and watersheds (W). Box plots include: median (horizontal line), 25% and 75% quantiles (box), and observations (circles). Shaded areas are the range of MI_{60} thresholds (T) that maximized the prediction accuracy (*F*) for each dataset.

Table 4
ANOVA results for T_{min} using four models: (1) plots, (2) hillslopes, (3) all spatial scales, and (4) all spatial scales with interactions. Data are degrees of freedom (DF) and p-values for T_{min}. Bold text indicates $p \leq 0.05$.

Model	Fixed effects	DF	p-value
Plot	Fire	1	0.11
	Year	4	0.06
	Mulch	1	0.85
Hillslopes	Fire	2	0.52
	Year	4	**0.02**
	Mulch	1	0.29
All Spatial scales	Fire	2	0.13
	Year	4	**0.01**
	Spatial scale	2	**0.01**
Year*Spatial scale	Year	4	0.18
	Spatial scale	2	**0.01**
	Year*Spatial scale	8	0.09

ANOVA analyses. This is probably because no fire had consistently higher or lower thresholds than the others (Table 3). For example, at unmulched hillslopes during post-fire years 0–1 Hayman T_{min} values were highest (9–11 mm h^{-1}), whereas during year 2 High Park T_{min} was highest (16 mm h^{-1}), and in year 3 Bobcat was highest (22 mm h^{-1}).

Year post-fire was a significant fixed effect in the first three ANOVA models (Table 4). For unmulched hillslopes, T_{min} in Bobcat fire was 7 mm h^{-1} for years 0–2 then increased to 21 mm h^{-1} in year 3. T_{min} at unmulched hillslopes in the Hayman fire was 8–11 mm h^{-1} for years 0–3 then increased to 21 mm h^{-1} in year 4. For unmulched hillslopes in the High Park fire, T_{min} increased from 4 mm h^{-1} in year 0 to 7 mm h^{-1} in year 1 and 12 mm h^{-1} in years 2–3. Overall, each of the fires exhibited increases in thresholds over time, but the timing of this increase varied between fires.

Spatial scale was also a significant fixed effect in the third and fourth ANOVAs (Table 4). The ANOVA models with subsequent multiple comparisons using Tukey's HSD indicate that T_{min} was significantly higher for hillslopes than either plots or watersheds, but this result may be misleading because half of the threshold at the watershed scale were low-confidence (Tables 3 and S2). In the Bobcat fire, T_{min} values were the same for plots and hillslopes (7 mm h^{-1}) in year 1, but increased from plot to hillslope scale (4–7 mm h^{-1}) in year 2; other years did not have high-confidence thresholds across multiple spatial scales. In the Hayman fire, for the years where T_{min} could be compared between scales, values increased from plot to hillslope scale (5–8 mm h^{-1}) in year 2 and stayed the same for plot and hillslope scale in year 3 (8 mm h^{-1}). In the High Park fire, the years with threshold predictions for both hillslopes and watersheds (years 2–3) did not have high-confidence thresholds at the hillslope scale. Lower thresholds for watersheds than plots or hillslopes may have been the result of antecedent precipitation, which was significantly higher (ANOVA; $p < 0.0001$) for rain storms with responses in runoff (average = 32 mm) as compared to those without (average = 22 mm).

3.3. Frequency of threshold exceedance

For the frequency analysis of threshold-exceeding MI_{60} summer rain storms, we focused on post-fire years 0–2 because thresholds tended to increase significantly after post-fire year 2 (Tables 3 and 4). Frequencies of threshold exceedance for a given summer were generally higher on the drier eastern slopes of the Front Range and lower for the forests in the western mountainous portion of Colorado (Fig. 5).

For the eastern slope of Colorado's Front Range, the frequency of threshold exceedance increased with increasing elevation from 1500 to 2100 m, decreased with increasing elevation from 2100 to 2300 m, and was relatively consistent above 2300 m (Fig. 6). Summer rain storms exceeding MI_{60} of 4 mm h^{-1}, the lower bound of high-confidence post-fire response thresholds for years 0–2, were estimated to occur from five to eleven times per typical summer (Fig. 5). Storms with an MI_{60} threshold of 8 mm h^{-1} were estimated to occur between two to five times per summer, and rainfall events with an MI_{60} threshold of 12 mm h^{-1} were estimated to occur between one to three times per summer (Fig. 5). The highest frequency for each threshold generally

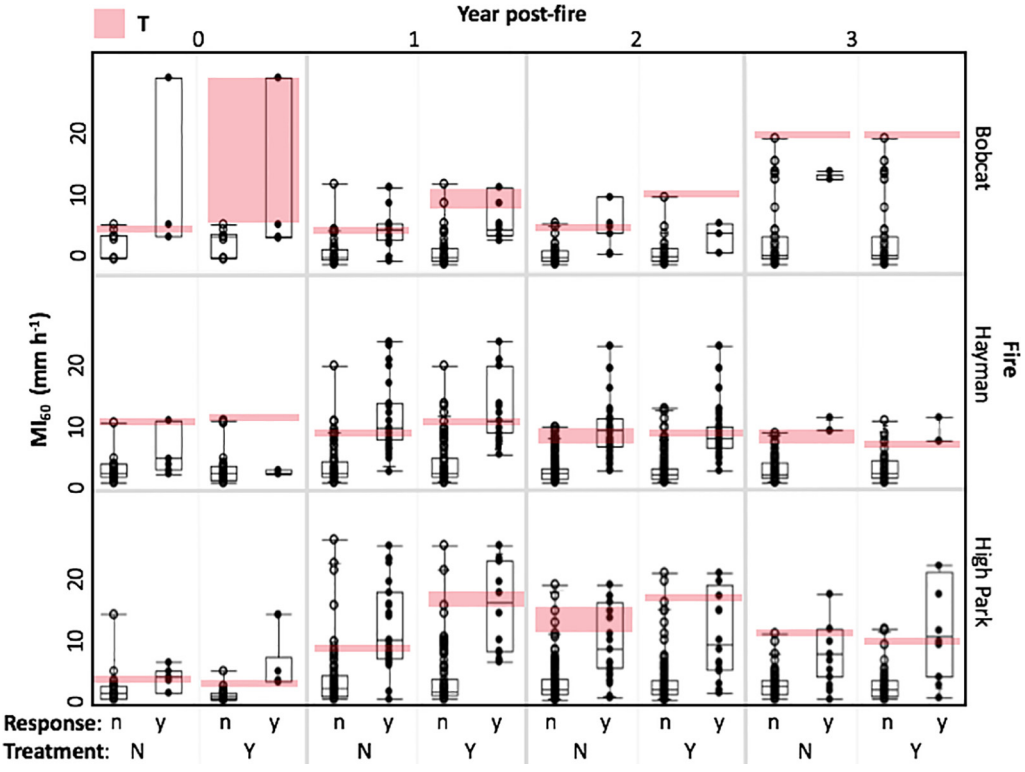

Fig. 4. MI_{60} rainfall and thresholds (T) for hillslopes by mulch treatment (N/Y), year post-fire, fire, and response absence (n; open circles) or presence (y; filled circles). Box plots include the median (horizontal line), 25% and 75% quantiles (box), and observations (circles). Shaded areas are the range of MI_{60} thresholds (T) that maximized the prediction accuracy (*F*) for each dataset.

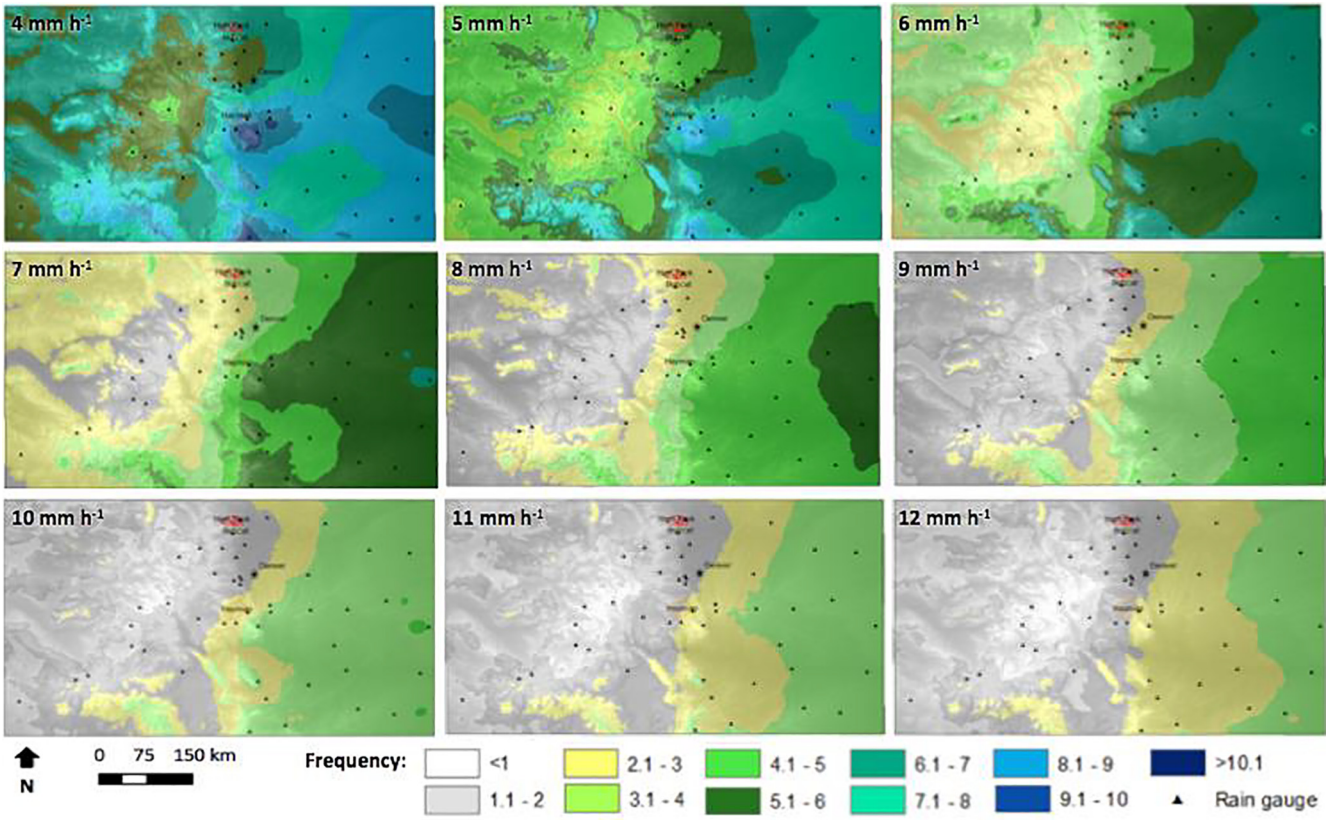

Fig. 5. Annual average June-September threshold exceedance frequencies for MI_{60} values of 4–12 mm h^{-1} across Colorado. The black triangles are the NOAA rain gauges with at least 25 years of 15-min data (Perica et al., 2013). Maps produced using GCS WGS 1984.

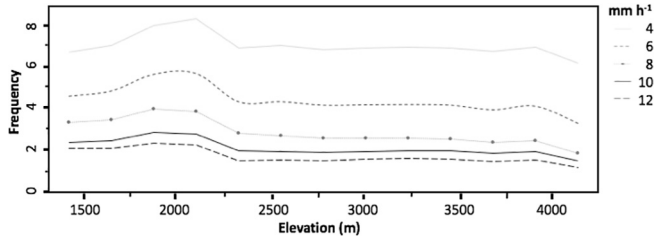

Fig. 6. Annual average June-September threshold exceedance frequencies by elevation for rainfall with MI_{60} values of 4 to 12 mm h^{-1} ion the eastern slope of Colorado's Front Range.

occurred just southeast of the Hayman fire (Fig. 5). Frequencies higher than 8 mm h^{-1} are greater than the range of high-confidence thresholds we identified for post-fire years 0–2 (4–8 mm h^{-1}), but we include them here to illustrate how frequencies change with increasing intensities.

4. Discussion

4.1. Relationship to other research

Rainfall thresholds for post-fire runoff and sediment delivery have been mentioned in previous research, but this is the first paper to rigorously identify and compare post-fire runoff and sediment delivery thresholds across multiple fires, years post-fire, spatial scales, and the presence or absence of mulch treatments. Most previous studies have reported thresholds as maximum 30-min rainfall intensity (MI_{30}) values. We related our MI_{30} values to MI_{60} values from the same storms, and found that these were strongly correlated (Eq. (6); n = 1296; Spearman's r = 0.97). The following linear fit equation allows us to compare our thresholds to those in the literature:

$$MI_{60} = 0.57MI_{30} + 0.13 \quad (6)$$

where all units are mm h^{-1}.

The conversion of published MI_{30} thresholds to MI_{60} values using Eq. (6) results in MI_{60} values that are very similar to our MI_{60} thresholds. Estimated MI_{60} thresholds for post-fire runoff in 220 to 2200 ha basins across the western US were 5 mm h^{-1} for post-fire years 0–1 and 6 mm h^{-1} for post-fire year 2 (Moody, 2002). The MI_{60} thresholds were 3–5 mm h^{-1} for post-fire years 1 and 2 in Spring Creek (260 ha) following the Buffalo Creek fire (Moody, 2002). In New Mexico's 2000 Cerro Grande fire, runoff was not generated in seven sub-watersheds (24 to 85 ha) until MI_{60} was at least 5 mm h^{-1} (Moody et al., 2008). After the 2010 Fourmile Canyon fire, hydrologic responses were primarily driven by MI_{60} > 6 mm h^{-1} (Murphy et al., 2016). These thresholds mostly fall within the 4–8 mm h^{-1} range of high-confidence MI_{60} thresholds that we identified for plots, hillslopes and watersheds of the Bobcat, Hayman and High Park fires in post-fire years 0–2.

We can also compare the increase in our MI_{60} thresholds over time with other studies. In our study, the unmulched hillslope data showed a progressive increase in thresholds from year 0 to year 2 in the High Park fire, a large increase in year 3 in the Bobcat fire, and a large increase in year 4 in the Hayman fire. The slower recovery in the Hayman fire has been noted previously and attributed to the very coarse granitic soils with low water holding capacity and poor nutrient status (e.g., Robichaud et al., 2013a,b; Wagenbrenner et al., 2015). The Buffalo Creek fire also has very coarse-textured granitic soils, and hillslope runoff and sediment delivery rates only decreased toward pre-fire conditions after 3-4 years post-fire (Moody and Martin, 2001a,b). Other Front Range fire studies have documented substantial recovery in terms of hillslope sediment production by the third summer after burning (Benavides-Solorio and MacDonald, 2005; Wagenbrenner et al., 2006). In other Rocky Mountain study areas, post-fire recovery of vegetation and ground cover occurred within 1–6 years after burning, while the

recovery of infiltration capacity occurred 2–3 years after burning (Ebel and Martin, 2017). This corresponds to the time needed for sufficient vegetation regrowth and litter accumulation to allow infiltration capacities of soils to exceed summer rainfall intensities.

4.2. Factors affecting thresholds

Our analyses highlighted similarities in thresholds across fires, increases in thresholds with year post-fire, and potential changes in thresholds with spatial scale. There are several important limitations to note in interpreting these results. First, post-fire infiltration rates and thresholds for post-fire surface runoff and sediment delivery are affected by high spatial and temporal variability in site characteristics. Previous studies have found that surface cover and soil sealing (Wainwright et al., 2000; Larsen et al., 2009; Moreno-de las Heras et al., 2010; Inbar et al., 1998), spatial scale (Cammeraat, 2002), flow path length (Wagenbrenner and Robichaud, 2014), soil type (Miller et al., 2011) and soil water repellency (Benavides-Solorio and MacDonald, 2001; Woods et al., 2007) are all important for post-fire response, but we did not have data on all of these factors for all study sites. Consequently, there may have been important factors affecting thresholds that we did not consider in the analyses. Second, given the differences in sample size across fires, years, and scales, our dataset was imbalanced, which made it difficult to isolate the effects of individual factors. Third, rainfall data contributed additional uncertainty to the analyses. Relating a specific storm to a response in runoff or sediment delivery is inherently uncertain if there are multiple storms between field visits to empty sediment fences. When multiple storms occurred between site visits, we attributed the response to the storm with the maximum EI_{30}. This potentially led to higher than expected thresholds if multiple storms produced sediment, and at least one of those storms was less intense than the one that was attributed to the observed response. In addition, some plots and hillslopes were more than a kilometer away from the nearest rain gauge. Summer convective storms can generate highly variable rainfall intensities with maximum rainfall depths occurring within 2500 m of the storm center (Osborn and Laursen, 1973). If higher rainfall intensities occurred at a given site compared to its nearest rain gauge, these sites would have an unrealistically low threshold response. The opposite problem, where a site had lower intensity rain than recorded by the nearest rain gauge, could lead to false positives. Finally, for each rain storm, the threshold analysis assigned binary responses of runoff or sediment delivery (i.e., presence or absence), excluding information on the magnitude of responses. For hillslopes, smaller sediment yields ($< 0.05\ Mg\ ha^{-1}$) accounted for 70% of responses (Fig. S1), and higher thresholds would likely be needed to predict larger production events.

Despite these limitations, our analysis draws on a large dataset to reveal which factors influence post-fire response thresholds, providing important insights about how fire affects runoff and sediment delivery. The factor that most consistently emerged as an important influence on thresholds was year post-fire. Scale was also a significant effect, but these results are not as straightforward to interpret. The data were easier to compare among plots and hillslopes because these inherently have less spatial variability than watersheds, and the plot and hillslope scales are also more easily replicated. The MI_{60} thresholds at the plot and hillslope scales were generally quite similar across all fires, likely because processes of overland flow generation and downslope connectivity are similar among plot and hillslope scales in areas of high burn severity. Watershed thresholds are more difficult to compare to one another because watersheds typically have much more spatial variability in burn severity, and a given thunderstorm will probably not be evenly distributed across a watershed (Kampf et al., 2016; Brogan et al., 2017). For our study, there was also very little temporal overlap in the years with watershed data or lowconfidence thresholds otherwise, so we could not rigorously compare watershed scale thresholds across fires. We found a lower MI_{60} for generating a response at the watershed scale than hillslope scale in the High Park fire (Table 3), but this was only in post-fire years 2–3 when threshold confidence was low for hillslopes. During these years, only 50% of the rain storms that caused a response at hillslopes also caused a watershed response. On the other hand, for nearly 20% of the rain storms, a runoff response was observed at watersheds when there was no response in sediment delivery at the monitored hillslopes. This may have been caused by storms with limited spatial extent or differences in antecedent precipitation. Antecedent precipitation was higher for rain storms with runoff than those without at watersheds within the High Park fire, potentially leading to increased water storage within the channel and riparian zones and lower MI_{60} thresholds to initiate a runoff response in watersheds. Concurrent monitoring of runoff across different spatial scales is needed for understanding when and how hillslope runoff connects to downstream areas.

We also aimed to examine the effects of mulching on thresholds, but this proved challenging because of differences in treatments and sample sizes between fires and scales. Mulch did not emerge as a significant source of differences for plot or hillslope scale thresholds in the ANOVA analyses, possibly because of limited sample sizes of mulched and unmulched sites across multiple fires and years. The biggest effect of mulching was to increase T_{min} at the hillslope scale, especially in the Bobcat and High Park fires in post-fire years 1 and 2 (Table 3). Mulching had little or no effect on the response thresholds at either the hillslope or plot scales in post-fire years 3 and 4. Previous studies have shown that mulching is most effective in reducing percent bare soil and sediment delivery compared to relatively bare unmulched sites; vegetation regrowth at both mulched and unmulched sites causes a progressively smaller effect of mulch over time (Wagenbrenner et al., 2006; Rough, 2007). It is surprising that mulch did not have much of an effect on the MI_{60} thresholds in the Hayman fire because mulch did cause a large reduction in erosion at the plot and hillslope scales in other studies (Rough, 2007; Robichaud et al., 2013b).

4.3. Frequency of threshold exceedance

The rainfall thresholds and frequency maps identified the likelihood of post-fire runoff and sediment delivery at plot, hillslope and watershed scales. Our results showed that Colorado's Front Range is likely to experience several (2–11) rain storms that exceed thresholds for generating post-fire responses each summer. The frequency maps were most reliable in areas with high NOAA Atlas station density, such as central and eastern Colorado, and least reliable in areas with fewer stations, such as northwestern Colorado. On the eastern slope of the Colorado Front Range, the peak frequency of high intensity storms was at an elevation near 2100 m. This indicates that burned areas near this elevation—like the three study fires—are also most susceptible to high intensity storms. Further analyses are needed to determine if the elevation dependence of the < 1 year recurrence interval storms we mapped is similar to spatial patterns of less frequent, more intense storms.

The frequency maps can be used by burned area emergency response (BAER) teams or emergency management organizations and water utilities to rapidly estimate the number of post-fire runoff or sediment delivery events that might occur in a typical summer. This information can be useful for land management, flood mitigation, and water treatment decisions. Our thresholds are relatively conservative in that not all threshold-exceeding events will generate a large response (Fig. S1). Additional monitoring is needed to determine how the responses at hillslope or small watershed scales relate to downstream impacts in larger rivers. The thresholds and frequencies we identified should also be adjusted as needed for specific site conditions, as some sites may have a slower revegetation rate, and therefore lower MI_{60} thresholds may persist over a longer time period.

4.4. Future work

A more robust threshold analysis would be possible with some changes and improvements in future post-fire data collection efforts. In particular, rain gauges must be carefully maintained and closely spaced (e.g., Osborn et al., 1972), especially in areas where convective storms are the main cause of post-fire runoff and erosion. At least annual measurements of post-fire ground cover should also be made to help explain the variability in response thresholds over time. Obtaining watershed scale ground cover data is difficult, so intensively monitored plots and hillslopes should be nested within monitored watersheds, with other sampling points added as needed to characterize ground cover at the watershed scale. Ground cover measurements could also be designed to inform remote sensing image classification for mapping cover across larger areas. These measurements would be particularly useful to evaluate the amount and persistence of mulch cover and effect on thresholds at the watershed scale. The applicability of our results also can be improved by collecting data across a wider range of climates and soils.

The rainfall thresholds identified here are related to the effective hydraulic conductivity of the domains sampled and could help calibrate and evaluate models that are currently being used to estimate post-fire runoff and erosion, such as disturbed WEPP (Elliot, 2004) and ERMiT (Robichaud et al., 2007). Our methods for determining thresholds and mapping frequencies of threshold exceeding rainfall events could be applied to other regions using region-specific data. Thresholds could also be adjusted to account for projected changes in the frequency and magnitude of rainfall intensities in future climate conditions.

5. Conclusions

This study identified rainfall intensity thresholds for post-fire runoff and sediment delivery at the plot, hillslope and watershed scales for three fires in the Colorado Front Range. The analysis focused on the summer thunderstorms that generate almost all of the post-fire responses at plots and hillslopes and the largest responses at watersheds. Considering all years post-fire, thresholds varied significantly among spatial scales and years post-fire, but insignificantly among fire locations and with mulch treatment. For the first three summers after burning (post-fire years 0–2), we have high confidence that runoff or sediment delivery were observed when maximum 60-min rainfall intensities exceeded 4 to 8 mm h^{-1}. On the eastern slope of the Colorado Front Range, storms at or exceeding this range of intensities will likely occur between two to eleven times in a typical summer. Areas most likely to generate post-fire runoff and erosion can be identified with the threshold exceedance frequency maps, which can aid rapid assessment of potential post-fire impacts to downstream residents, infrastructure and water supplies.

Acknowledgements

This work was supported by a Joint Fire Science Graduate Research Innovation Award (Project #: 15-2-01-57) and National Science Foundation Grant No. DGE-0966346 “I-WATER: Integrated Water, Atmosphere, Ecosystems Education and Research Program” at Colorado State University. Data collection from the High Park Fire was also supported by the City of Greeley and by National Science Foundation grants DIB-1230205 and DIB-1339928, while data collection from the other fires was supported by a wide range of grants, particularly by the affected national forests and the USDA Forest Service Rocky Mountain Research Station and the USDA-US Forest Service Joint Fire Science Program. We thank Sandra Ryan, Matt Kunze, Pete Robichaud, Isaac Larsen, and many other researchers and field personnel for collecting the data that made this analysis possible. We also thank Clayton Bliss for his assistance with data analysis. Two anonymous reviewers provided very useful comments that improved and clarified this manuscript.

Appendix A. Supplementary material

Supplementary data associated with this article can be found, in the online version, at https://doi.org/10.1016/j.foreco.2018.08.025.

References

ARS (Agriculture Research Service), 2013. Rainfall Intensity Summarization Tool (RIST) (Version 3.89) [computer software]. United States Department of Agriculture. Retrieved from <http://www.ars.usda.gov/Research/docs.htm?docid=3251>.
Benavides-Solorio, J.D., MacDonald, L.H., 2001. Post-fire runoff and erosion from simulated rainfall on small plots, Colorado Front Range. Hydrol. Process. 15, 2931–2952.
Benavides-Solorio, J.D., MacDonald, L.H., 2005. Measurement and prediction of post-fire erosion at the hillslope scale, Colorado Front Range. Int. J. Wildland Fire 14, 1–18.
Braddock, W.A., Nutalaya, P., Gawarecki, S.J., Curtin, G.C., 1970. Geologic map of the Drake Quadrangle, Larimer County, Colorado. US Department of Interior Geological Survey May GQ-829. USDI Geological Survey, Washington, DC.
Brogan, D.J., Nelson, P.A., MacDonald, L.H., 2017. Reconstructing extreme post-wildfire floods: a comparison of convective and mesoscale events. Earth Surf. Process. Landforms 42, 2505–2522.
Burned Area Emergency Response (BAER), 2012. High Park fire Burned Area Emergency Response Report. Colorado Dept. of Transportation, Larimer County, NRCS, and USDA, pp. 35.
Cammeraat, L.H., 2002. A review of two strongly contrasting geomorphological systems within the context of scale. Earth Surf. Process. Landforms 27, 1201–1222.
Cammeraat, L.H., 2004. Scale dependent thresholds in hydrological and erosion response of a semi-arid catchment in southeast Spain. Agric. Ecosyst. Environ. 104, 317–332.
Dingman, S.L., 2002. Physical Hydrology, second ed. Prentice-Hall Inc.
Ebel, B.A., Martin, D.A., 2017. Meta-analysis of field-saturated hydraulic conductivity recovery following wildland fire: applications for hydrologic model parameterization and resilience assessment. Hydrol. Process. 31, 3682–3696.
Elliot, W.J., 2004. WEPP internet interfaces for forest erosion prediction. J. Am. Water Resour. Assoc. 40 (2), 299–309. https://doi.org/10.1111/j.1752-1688.2004.tb01030.x.
ESRI, 2013. ArcGIS Desktop: Release 10.2. Environmental Systems Research Institute, Redlands, CA.
Hohner, A.K., Cawley, K., Oropeza, J., Summers, R.S., Rosario-Ortiz, F.L., 2016. Drinking water treatment response following a Colorado wildfire. Water Res. 105, 187–198.
Inbar, M., Tamir, M., Wittenberg, L., 1998. Runoff and erosion processes after a forest fire in Mount Carmel, a Mediterranean area. Geomorphology 24, 17–33.
JMP®, Version 12.0.1. SAS Institute Inc., Cary, NC, 1989-2007.
Kampf, S.K., Brogan, D.J., Schmeer, S., MacDonald, L.H., Nelson, P.A., 2016. How do geomorphic effects of rainfall vary with storm type and spatial scale in a post-fire landscape? Geomorphology 273, 39–51.
Kutiel, P., Lavee, H., Segev, M., Benyamini, Y., 1995. The effect of fire-induced heterogeneity on rainfall-runoff-erosion relationships in an eastern Mediterranean ecosystem, Israel. Catena 25, 77–87.
Kunze, M.D., Stednick, J.D., 2006. Streamflow and suspended sediment yield following the 2000 Bobcat fire, Colorado. Hydrol. Process. 20, 1661–1681.
Larsen, I.J., MacDonald, L.H., Brown, E., Rough, D., Welsh, M.J., Pietraszek, J.H., Libohova, Z., Benavides-Soorio, Jd.D., Schaffrath, K., 2009. Causes of post-fire runoff and erosion: water repellency, cover, or soil sealing? Soil Sci. Soc. Am. J. 73, 1393–1407.
Litschert, S.E., Brown, T.C., Theobald, D.M., 2012. Historic and future extent of wildfires in the Southern Rockies Ecoregion, USA. For. Ecol. Manage. 269, 124–133.
Martin, D.A., 2016. At the nexus of fire, water and society. Phil. Trans. R. Soc. B. 371, 20150172. https://doi.org/10.1098/rst.2015.0172.
Miller, M.E., MacDonald, L.H., Robichaud, P.R., Elliot, W.J., 2011. Predicting post-fire hillslope erosion in forest lands of the western United States. Int. J. Wildland Fire 20, 982–999.
Moody, J.A., Martin, D.A., 2001a. Initial hydrologic and geomorphic response following a wildfire in the Colorado Front Range. Earth Surf. Process. Landforms 26, 1049–1070.
Moody, J.A., Martin, D.A., 2001b. Post-fire rainfall intensity-peak discharge relations for three mountainous watersheds in the western USA. Hydrol. Process. 15, 2981–2993.
Moody, J., 2002. An Analytical Method for Predicting Post-wildfire Peak Discharges. U.S. Geological Survey Scientific Investigations Report 2011-5236, 36 p.
Moody, J.A., Martin, D.A., Haire, S.L., Kinner, D.A., 2008. Linking runoff response to burn severity after a wildfire. Hydrol. Process. 22, 2063–2074.
Moody, J.A., Shakesby, R.A., Robichaud, P.R., Cannon, S.H., Martin, D.A., 2013. Current research issues related to post-wildfire runoff and erosion processes. Earth Sci. Rev. 122, 10–37.
Moreno-de las Heras, M., Nicolau, J.M., Merino-Martin, L., 2010. Plot-scale effects on runoff and erosion along a slope degradation gradient. Water Resour. Res. 46, W04503. https://doi.org/10.1029/2009WR007875.
Murphy, S.F., Writer, J.H., McCleskey, R.B., Martin, D.A., 2016. The role of precipitation type, intensity, and spatial distribution in source water quality after wildfire. Environ. Res. Lett. 10, 08400.
Noske, P.J., Nyman, P., Lane, P.N.J., Sheridan, G.J., 2016. Effects of aridity in controlling the magnitude of runoff and erosion after wildfire. Water Resour. Res. 52, 4338–4357. https://doi.org/10.1002/2015WR017611.
Nyman, P., Sheridan, G.J., Lane, P.N., 2013. Hydro-geomorphic response models for

burned areas and their applications in land management. Prog. Phys. Geogr. 37, 787–812.
Osborn, H.B., Lane, L.J., Hundley, J.F., 1972. Optimum gaging of thunderstorm rainfall in southeastern Arizona. Water Resour. Res. 8 (1), 259–265.
Osborn, H.B., Laursen, E.M., 1973. Thunderstorm runoff in southeastern Arizona. J. Hydraul. Div. 99 (HY7), 1129–1145.
Perica, S., Martin, D., Pavlovic, S., Roy, I., St. Laurent, M., Trypaluk, C., Unruh, D., Yekta, M., Bonnin, G., 2013. NOAA Atlas 14 Volume 8 Version 2, Precipitation-Frequency Atlas of the United States, Midwestern States. NOAA, National Weather Service, Silver Spring, MD.
PRISM Climate Group, Oregon State University. 2017. <http://www.prism.oregonstate.edu/normals/> (accessed 5 July 2017).
Renard, K.G., Foster, G.R., Weesies, G.A., McCool, D.K., Yoder, D.C., 1997. Predicting Soil Erosion by Water: A Guide to Conservation Planning with the Revised Universal Soil Loss Equation (RUSLE). Agriculture Handbook Number 703. Agricultural Research Service. U.S. Department of Agriculture, Washington D.C.
Robichaud, P.R., Brown, R.E., 2002. Silt Fences: An Economical Technique for Measuring Hillslope Soil Erosion. Gen. Tech. Rep. RMRS-GTR-94. U.S. Department of Agriculture, Forest Service, Rocky Mountain Research Station, Fort Collins, CO, 24 p.
Robichaud, P.R., Elliot, W.J., Pierson, F.B., Hall, D.E., Moffet, C.A., 2007. Predicting postfire erosion and mitigation effectiveness with a web-based probabilistic erosion model. Catena 71, 229–241.
Robichaud, P.R., Wagenbrenner, J.W., Brown, R.E., Wohlgemuth, P.M., Beyers, J.L., 2008. Evaluating the effectiveness of contour-felled log erosion barriers as a post-fire runoff and erosion mitigation treatment in the western United States. Int. J. Wildland Fire 17 (2), 255–273. https://doi.org/10.1071/Wf07032.
Robichaud, P.R., Jordan, P., Lewis, S.A., Wagenbrenner, J.W., Ashmun, L.E., Brown, R.E., 2013a. Post-fire mulching for runoff and erosion mitigation Part I: effectiveness at reducing hillslope erosion rates. Catena 105, 75–92.
Robichaud, P.R., Wagenbrenner, J.W., Lewis, S.A., Ashmun, L.E., Brown, R.E., Wohlgemuth, P.M., 2013b. Post-fire mulching for runoff and erosion mitigation Part II: effectiveness in reducing runoff and sediment yields from small catchments. Catena 105, 93–111.
Rough, D., 2007. Effectiveness of Rehabilitation Treatments in Reducing Post-fire Erosion After the Hayman and Schoonover Fires, Colorado Front Range (MS thesis). Colorado State University.
Schmeer, S.R., 2014. Post-fore Erosion Response and Recovery, High Park Fire, Colorado (MS thesis). State University, Colorado.
Schmeer, S.R., Kampf, S.K., MacDonald, L.H., Hewitt, J., Wilson, C., 2018. Empirical models of annual post-fire erosion on mulched and unmulched hillslopes. Catena 163, 276–287.
Veblen, T.T., Kitzberger, T., Donnegan, J., 2000. Climatic and human influences on fire regimes in Ponderosa Pine forests in the Colorado Front Range. Ecol. Appl. 10 (4), 1178–1195.
Viera, A.J., Garrett, J.M., 2005. Understanding interobserver agreement: the kappa statistic. Fam. Med. 37 (5), 360–363.
Wagenbrenner, J.W., MacDonald, L.H., Rough, D., 2006. Effectiveness of three post-fire rehabilitation treatments in the Colorado Front Range. Hydrol. Processes. 20, 2989–3006.
Wagenbrenner, J.W., Robichaud, P.R., 2014. Post-fire bedload sediment delivery across spatial scales in the interior western US. Earth Surface Proc. Landforms. 39, 865–876.
Wagenbrenner, J.W., MacDonald, L.H., Coats, R.N., Robichaud, P.R., Brown, R.E., 2015. Effects of post-fire salvage logging and a skid trail treatment on ground cover, soils, and sediment production in the interior western United States. For. Ecol. Manage. 335, 176–193. https://doi.org/10.1016/j.foreco.2014.09.016.
Wainwright, J., Parsons, A.J., Abrahams, A.D., 2000. Plot-scale studies of vegetation, overland flow and erosion interactions: case studies from Arizona and New Mexico. Hydrol. Process. 14, 2921–2943.
Westerling, A.L., Hidalgo, H.G., Cayan, D.R., Sweetnam, T.W., 2006. Warming and earlier spring increase U.S. forest wildfire activity. Science 313, 940–943.
Woods, S.W., Birkas, A., Ahl, R., 2007. Spatial variability of soil hydrophobicity after wildfires in Montana and Colorado. Geomorphology 86, 465–479. https://doi.org/10.1016/j.geomorph.2006.09.015.